Molecular Medicine

RESEARCH ARTICLE Open Access

Age-related decline in melatonin contributes to enhanced osteoclastogenesis via disruption of redox homeostasis

Di-Zheng Wu[1†], Guo-Zheng Zhu[1†], Kai Zhao[2†], Jia-Wen Gao[1], Gui-Xing Cai[1], Hong-Zhou Li[1], Yu-Sheng Huang[1], Chen Tu[1], Jing-Shen Zhuang[1], Zhi-Wei Huang[1] and Zhao-Ming Zhong[1*]

Abstract

Background Increased oxidative stress contributes to enhanced osteoclastogenesis and age-related bone loss. Melatonin (MT) is an endogenous antioxidant and declines with aging. However, it was unclear whether the decline of MT was involved in the enhanced osteoclastogenesis during the aging process.

Methods The plasma level of MT, oxidative stress status, bone mass, the number of bone marrow-derived monocytes (BMMs) and its osteoclastogenesis were analyzed in young (3-month old) and old (18-month old) mice (n = 6 per group). In vitro, BMMs isolated from aged mice were treated with or without MT, followed by detecting the change of osteoclastogenesis and intracellular reactive oxygen species (ROS) level. Furthermore, old mice were treated with MT for 2 months to investigate the therapeutic effect.

Results The plasma level of MT was markedly lower in aged mice compared with young mice. Age-related decline in MT was accompanied by enhanced oxidative stress, osteoclastogenic potential and bone loss. MT intervention significantly suppressed the receptor activator of nuclear factor-κB ligand (RANKL)-induced osteoclastogenesis, decreased intracellular ROS and enhanced antioxidant capacity of BMMs from aged mice. MT supplementation significantly attenuated oxidative stress, osteoclastogenesis, bone loss and deterioration of bone microstructure in aged mice.

Conclusions These results suggest that age-related decline of MT enhanced osteoclastogenesis via disruption of redox homeostasis. MT may serve as a key regulator in osteoclastogenesis and bone homeostasis, thereby highlighting its potential as a preventive agent for age-related bone loss.

Keywords Aging, Bone loss, Melatonin, Osteoclastogenesis, Osteoporosis, Oxidative stress

†Di-Zheng Wu, Guo-Zheng Zhu and Kai Zhao are co-first authors and contributed equally.

*Correspondence:
Zhao-Ming Zhong
zhongzm@smu.edu.cn
Full list of author information is available at the end of the article

Introduction

Bone mass is maintained by continuous remodeling through a coupled process of bone resorption and bone formation (Compston et al. 2019). With age, bone resorption slowly begins to exceed new bone formation, which causes gradual loss of bone mass and deterioration of bone microstructure, leading ultimately to the development of osteoporosis (Cui et al. 2022). Bone resorption is carried out by osteoclasts, which are multinucleated cells formed by fusion of monocyte/macrophage precursors. The formation of osteoclasts, also called osteoclastogenesis, is a multi-stage process, including cell commitment, cell–cell fusion, and maturation (Moller et al. 2020; Jevon et al. 2002). Osteoclastogenesis is highly regulated by various endogenous and exogenous molecules, including reactive oxygen species (ROS) (Lee et al. 2005; Li et al. 2021). Aging is generally accompanied by the excess accumulation of ROS and oxidative stress, which contribute to enhanced osteoclastogenesis and bone loss (Manolagas. 2010). It is well established that scavenging ROS and alleviating oxidative stress are beneficial for suppressing of osteoclastogenesis and alleviating age-related bone loss (Zhuang et al. 2021; Liu et al. 2019).

Melatonin (MT) is a neurohormone secreted mainly by the pineal gland with the highest levels during the dark phase and negligible levels during the light phase (Li et al. 2019). Apart from the well-known circadian rhythms regulation, MT serves as a most potent endogenous antioxidant and plays a pivotal role in maintaining redox homeostasis (Galano et al. 2018; Rodriguez et al. 2004; Veneroso et al. 2009; Peyrot et al. 2008; Deng et al. 2006). Peak level of MT declines with aging and coincides with the age-related impairment of antioxidant potential (Rasmussen et al. 2001). It is well demonstrated that MT supplementation can improve antioxidant defense functions in both human and experimental animals (Kedziora-Kornatowska et al. 2008; Chen et al. 2020). Evidence has also suggested that MT may influence skeletal growth and bone formation (Li et al. 2019). MT treatment at pharmacological doses increases bone mass by increased bone formation and reduced bone resorption in vivo (Satomura et al. 2007; Munmun et al. 2021), and suppresses osteoclastogenesis through the attenuation of intracellular ROS in vitro (Zhou et al. 2017). Therefore, it is important to understand the role of MT as an antioxidant in regulating bone homeostasis.

Previous studies have demonstrated that reduced MT secretion is associated with many age-related diseases and pathological situations (Fishbein et al. 2021). The decline of MT may contribute to enhanced osteoclastogenesis and age-related bone loss, but this possibility hasn't been thoroughly investigated. Here, we reported that age-related decline of MT is associated with increased oxidative stress, osteoclastogenesis and bone loss, and MT can inhibit osteoclastogenesis by enhanced antioxidant capacity both in vivo and in vitro. MT supplementation may provide potential benefits for age-related bone loss.

Materials and methods

Animals, reagents, and antibodies

All animals were purchased from the Southern Medical University Experimental Animal Centre (Guangzhou, China). Animal procedures were conducted in accordance with the National Institutes of Health guidelines for the care and use of experimental animals and were approved by the Southern Medical University Institutional Animal Care and Use Committee. The 18-month-old C57BL/6 mice were used as an animal model of age-related osteoporosis (Shao et al. 2022). Young mice (3 month-old) were used as controls. In some experiments, the aged mice were injected intraperitoneally with or without MT (50 mg/kg/day) for 2 months (Khan et al. 2017; Ma et al. 2020). There were 6 mice in each group. Experimental mice were housed under the standard specific pathogen-free conditions with a 12 h light/12 h dark cycle at 20 ± 2 °C. After 24 h of the last MT injection, the mice were euthanized, blood samples were collected in a centrifuge tube with anticoagulant (heparin) at 10:00–11:00 AM, and the plasma was isolated and examined using ELISAs. After the femurs were dissected, some of them were frozen in liquid nitrogen for protein extractions. The remaining femur were stabilized in 4% paraformaldehyde for subsequent micro-computed tomography (CT) scanning, and tartrate-resistant acid phosphatase (TRAP) staining.

Receptor activator of nuclear factorκB ligand (RANKL) and macrophage colony stimulating factor (M-CSF) were purchased from PeproTech (Rocky Hill, NJ, USA). Fetal bovine serum (FBS), alpha minimum essential medium (α-MEM), penicillin, streptomycin, trypsin-ethylenediaminetetraacetic acid (Trypsin/EDTA), 4′,6-diamidino-2-phenylindole (DAPI), protease inhibitor tablets, horseradish peroxidase-conjugated secondary antibodies, SuperSignal West Pico Substrate, and CLXPosure Film were purchased from Gibco Thermo Fisher Scientific (Waltham, MA, USA). MT, dimethyl sulfoxide (DMSO), phosphate buffered saline (PBS), paraformaldehyde, bovine serum albumin (BSA), Triton X-100, and 2′,7′-dichlorofluorescein diacetate (DCFH2-DA) were obtained from Sigma-Aldrich (St. Louis, MO, USA). Stock solution of MT was prepared by dissolving in DMSO to the concentration of 500 mM and diluting in α-MEM to different concentrations as specified in individual experiments.

Isolation and culture of primary bone marrow-derived monocytes (BMMs)

Primary BMMs were isolated from the femurs and tibias of C57BL/6 mice. After dissecting aseptically under a laminar airflow hood, the ends of the bones were cut off with scissors and the marrow cells were flushed out using a sterile needle and syringe containing α-MEM. Red blood cells were removed by treatment with red blood cell lysis buffer (Beyotime Institute of Biotechnology, Haimen, China). After washing, the cells were cultured in α-MEM containing 10% FBS, 100 U/mL penicillin, and 100 μg/mL streptomycin at 37 °C with 5% CO_2 in 60-mm cell culture dishes. After incubating overnight, the cell suspension was collected and re-cultured in a complete medium supplemented with 100 ng/mL M-CSF. After a 3-day culture, non-adherent cells were removed by washing with PBS and the adherent cells were cultured until they reached 90% confluence. In subsequent experiments, BMMs were counted and seeded at 5000 cells per well in 96-well plates and 10,000 cells per well in 48-well plates. To observe cell morphology, bright field images of monocytes were collected using a Zeiss Axiovert 40 CFL phase contrast microscope (Carl Zeiss Ltd., Oberkochen, Germany).

Assay of cell proliferation

Cell proliferation of BMMs was evaluated using the Cell Counting Kit-8 (CCK-8; Beyotime). Ten microliters of the CCK-8 solution were added to each well in 96-well plates and cells were incubated for 1 h at 37 °C. Absorbance was determined at 450 nm using a microplate spectrophotometer (BioTek, Winooski, VT, USA).

In vitro osteoclast differentiation

BMMs were induced toward osteoclasts by plating 5×10^4 cells per well in a 24-well tissue culture plate and incubating with osteoclast differentiation media (α-MEM containing 10% FBS, 100 U/mL penicillin, 100 μg/mL streptomycin, 20 ng/mL M-CSF, and 50 ng/mL RANKL). Cells were cultured for 5 days with a change of culture media and cytokine supplementation every other day.

Bone resorption assay

In vitro, BMMs were seeded on bovine cortical bone slices (6×6 mm size and 0.2 mm thickness) and were treated as described above. After 6 days, adherent cells were removed and the bone slices were scanning electron microscopy (Hitachi S-3000N, Japan) to observe the bone resorption pits.

Flow cytometry and cell sorting

Cells were simultaneously stained for CD11b (PerCP-Cy5.5-conj., cloneM1/70), Ly6-G (Brilliant Violet650-conj., cloneRB6-8C5, all eBioscience) and Ly6-C (eFluor-conj., cloneAL-21). BMMs were characterized as $CD11b^{+}Ly6C^{+}Ly6G^{-}$. For flow-cytometric analyses, we used a BD FACSCanto II (Becton Dickinson Immunocytometry Systems, San Jose, CA, USA). For cell sorting, Monocytes from mice were stained with CD11b, Ly6C and Ly6G antibodies and then isolated using a BD FACSAria II sorter.

Micro-CT scanning

The bilateral femur was fixed with 4% PFA for 24 h and then scanned with a Micro-CT system (μCT80, SCANCO MEDICAL, Switzerland) as in our previous research (Zhu et al. 2018). Bone mineral density (BMD), bone volume over total volume (BV/TV), trabecular thickness (Tb/Vt.Th), trabecular number (Tb/Vt.N) and trabecular spacing (Tb/Vt.Sp), were calculated using the CTAn software.

Measurement of intracellular reactive oxygen species (ROS)

Intracellular levels of ROS were quantified by using a 2′,7′-dichlorofluorescein diacetate (DCFH2-DA) method. Monocytes were washed once with PBS and then incubated in α-MEM containing 50 μM DCFH2-DA at 37 °C for 30 min. After washing, cells were treated with MT at 100 μM. To investigate the role of ROS in osteoclastogenesis, cells were incubated in osteoclastogenic differentiation media supplemented with 100 μM MT. Fluorescence of the samples was measured at 488 nm excitation/525 nm emission by a SynergyMx multimode microplate reader (BioTek).

Tartrate-resistant acid phosphatase (TRAP) staining

Osteoclasts were washed twice with PBS, fixed with 4% paraformaldehyde for 15 min, and stained with a Leukocyte Acid Phosphatase Kit (Sigma-Aldrich) according to the manufacturer's instructions. After rinsing with deionized water, the fixed cells were incubated with Fast Garnet GBC Base solution (7.0 mg/mL in 0.4 mol/L hydrochloric acid) and sodium nitrite solution (0.1 mol/L) for 2 min. The cells were then stained with a mixture of naphthol AS-BI phosphate solution (12.5 mg/mL) and tartrate solution (0.335 mol/L, pH = 4.9 ± 0.1) in acetate buffer (2.5 mol/L, pH = 5.2 ± 0.1) in the dark for 10 min at 37 °C. The nuclei were counterstained with DAPI. Digital images of red-stained osteoclasts were captured by an Olympus IX51 microscope (Olympus Corporation, Tokyo, Japan). Multinucleated TRAP-positive

cells with more than three nuclei were counted as osteoclasts. The number of TRAP-positive osteoclasts and the number of nuclei within these osteoclasts were counted in ten randomly chosen fields of view (FOV).

Western blot analysis

Cells were dissolved in ice-cold cell lysis buffer (Beyotime) containing protease inhibitors; the protein concentration in cell extracts was quantified using a BCA protein assay kit (Beyotime). Equal amounts of protein from each extract were denatured and separated in a 10% polyacrylamide gel (Beyotime) and transferred by electrophoresis onto a nitrocellulose membrane (Thermo Fisher Scientific). The membrane was incubated with diluted primary antibodies against TRAP (#32694, 1:1000, SAB), cathepsin K(CTSK) (11239-1-AP, 1:1000, Proteintech), c-Fos (66590-1-Ig, 1:1000, Proteintech), NFATc1 (66963-1-Ig, 1:2000, Proteintech), NF-κB p65 (10745-1-AP, 1:1000, Proteintech), phospho-p65(ab76302, 1:1000, Abcam), IκB-α (51066-1-AP, 1:1000, Proteintech), phospho-IκB-α(ab133462, 1:10000, Abcam), Nrf2 (16396-1-AP, 1:5000, Proteintech), Keap1 (10503-2-AP, 1:2000, Proteintech), HO1 (10701-1-AP, 1:1000, Proteintech), or GAPDH (10494-1-AP, 1:10000, Proteintech) at 4 °C overnight, followed by the secondary antibody of horseradish peroxidase-conjugated goat anti-mouse or anti-rabbit for 1 h at room temperature. SuperSignal West Pico Substrate and CLXPosure Film were used for exposure. The intensity of the bands was quantified using the ImageJ software.

Immunofluorescence staining

An immunofluorescence staining was used to determine the effects of MT on the expression of Nrf2 and the nuclear translocation of P65. The control group and MT-treated monocytes were fixed with 4% paraformaldehyde for 15 min. Then permeabilized the cells with 0.3% Triton X-100 for 5 min and blocked with 3% BSA in PBS. The cells were incubated with anti-P65 or anti-Nrf-2 antibody followed by biotinylated goat anti-rabbit IgG antibody and fluoresce in conjugated streptavidin (Vector Laboratories, CA, USA).

Quantitative real-time polymerase chain reaction (qRT-PCR)

Total RNA was extracted using the TRIzol® reagent (Thermo Fisher Scientific) and reversely transcribed to complementary DNA (cDNA) by the RevertAid FirstStrand cDNA Synthesis Kit (Thermo Fisher Scientific). Quantitative real-time reverse transcription-polymerase chain reaction (qRT-PCR) was performed on a CFX96™ Real-Time PCR System (Bio-Rad) using the iTap™ Universal SYBR® Green Supermix kit (Bio-Rad, Hercules, CA, USA) according to the manufacturer's protocol. Relative transcript levels of target genes were calculated using the comparative Ct ($2-\Delta\Delta Ct$) method and expressed as a fold change respective to the control. The primer sequences are listed in Table 1.

Table 1 The sequences of primers used for qRT-PCR

GAPDH-F	AGGTCGGTGTGAACGGATTTG
GAPDH-R	TGTAGACCATGTAGTTGAGGTCA
TRAP-F	ACTTGCGACCATTGTTAGCC
TRAP-R	AGAGGGATCCATGAAGTTGC
CTSK-F	AGCAGAACGGAGGCATTGACTC
CTSK-R	TTTAGCTGCCTTTGCCGTGGC

Enzyme-linked immunosorbent assay (ELISA)

Each blood sample was centrifuged at 3000 rpm and 4 °C for 15 min and the plasma supernatant was removed and placed in a fresh centrifuge tube. The levels of melatonin (MT), advanced oxidative protein products (AOPPs), malondialdehyde (MDA) and superoxide dismutase-1 (SOD-1) were quantified using the respective ELISA kits, in accordance with the manufacturer's instructions. Absorbance at 450 nm was measured using a microplate reader (S/N 415-2687, Omega Bio-Tek, Ortenberg, Germany).

Statistical analysis

Statistical analysis was conducted using the SPSS 13.0 statistical software (SPSS Inc., Chicago, IL, USA). All data were expressed as means ± standard deviation (S.D.). The Shapiro–Wilk test was used to analyze the normality and equal distribution of variance between the different groups. For data with normal distribution, statistical analyses were performed with Student's t-test or ANOVA analyses of variance unless otherwise stated. Significance was indicated by a p-value.

Results

Decline of MT was accompanied by the enhanced osteoclastogenic potential and oxidative stress in the aging process

To address the age-related changes in MT level and osteoclastogenesis, the plasma levels of MT and oxidative stress markers were measured, the osteoclastogenic potential and bone microstructure were also detected. When compared with young mice, aged mice exhibited a sharp decline in the plasma level of MT (Fig. 1A), corresponding to a significant increase in oxidative stress markers, such as AOPPs, MDA (Fig. 1B, C) and a decrease in SOD-1(Fig. 1D). The expression of bone resorption markers, TRAP and CTSK, were higher in femoral metaphysis of aged mice than that in young mice (Fig. 1E–G).

A significantly higher number of TRAP-positive multinucleated cells was shown in the femoral metaphysis from aged mice compared with the young mice (Fig. 1H, I). A marked increase in the number of monocytes in the bone marrow cavity was also observed in aged mice (Fig. 1J, K). Furthermore, in vitro assay showed that the level of intracellular ROS was significantly higher in BMMs from aged mice than that in young mice (Fig. 1L). The BMMs from aged mice also showed a higher capacity of differentiation into TRAP-positive multinucleated cells (Fig. 1M, N) and F-actin ring formation (Fig. 1O). Moreover, compared with young mice, aged mice showed a loss of bone mass, deterioration of bone microstructure and cortical bone thinning in the aging process (Fig. 2). The above data indicated that a decline of MT level was associated with the enhanced osteoclastogenesis and oxidative stress in the aging process.

MT suppressed osteoclastogenesis of BMMs from aged mice

In order to investigate the effects of MT on osteoclastogenesis in vitro, BMMs from aged mice were cultured in the presence of M-CSF and RANKL with or without MT. First, we found that MT of 100 μM had an inhibitory effect on intracellular ROS production and osteoclastogenesis, but no significant effect on cell proliferation, and was therefore used as the optimal drug concentration (Additional file 1: Fig. S1). MT treatment significantly decreased TRAP positive multinuclear cells (Fig. 3A, B) and inhibited the formation of F-actin ring (Fig. 3C). MT treatment also inhibited the gene and protein expression of osteoclast differentiation markers, such as TRAP and CTSK (Fig. 3D–G). The bone resorption pits assay showed that MT treatment significantly inhibited the bone resorption activity of osteoclasts (Fig. 3H). Previous studies showed that NFATc1, c-Fos and NF-κB were considered important regulators regulators for osteoclastogenesis (Kim et al. 2014; Ni et al. 2020). MT treatment also inhibited the expression of c-fos and NFATc1 expression (Fig. 3I–K). As shown in Fig. 4A–F, following RANKL stimulation, phosphorylation of IκB and p65 was enhanced in BMMs from aged mice compared to young mice, and translocation of p65 from the cytoplasm to the nucleus was also increased, Importantly, this above process was inhibited by MT treatment.

MT enhanced antioxidant capacity of BMMs from aged mice

ROS accumulation and oxidative stress contribute to enhanced osteoclastogenesis (Lee et al. 2005). As shown in Fig. 5A, BMMs from aged mice had higher intracellular ROS level than BMMs from young mice, but MT treatment significantly decreased the intracellular ROS level. Under excessive ROS accumulation conditions, some antioxidant enzymes are activated to resist oxidative stress. Keap1/ nuclear factor erythroid 2-related factor 2 (Nrf2) pathway has been regarded as the main signaling cascade regulating the activation of antioxidant enzymes, including heme oxygenase (HO)-1 (Kanzaki et al. 2017; Hyeon et al. 2013). MT treatment significantly increased the expression of Nrf2, Keap1 and HO-1 in BMMs of aged mice (Fig. 5B–F), which indicates that MT enhanced the antioxidant capacity of BMMs.

MT supplement attenuated oxidative stress and osteoclastogenesis in aged mice

To further determine the effects of MT on osteoclastogenesis in vivo, aged mice were intraperitoneally injected with MT (50 mg/kg/day) for 2 months. As shown in Fig. 6A, the MT supplementation significantly increased the plasma MT level in aged mice. As shown in Fig. 6B–D, the plasma oxidative stress markers, such as AOPPs and MDA, were decreased and SOD-1 was increased after exogenous MT treatment. BMMs also were isolated from MT treated mice and used to analyze the intracellular ROS level. As shown in Fig. 6G, there was a lower intracellular ROS level in BMMs from aged mice with MT treatment compared with aged mice. Furthermore, when aged mice received MT, the number of BMMs in the bone marrow cavity was markedly decreased (Fig. 6E, F). The expression of TRAP and CTSK (Fig. 6H–J) as well as TRAP positive cells (Fig. 6K,

(See figure on next page.)

Fig. 1 The decline of melatonin (MT) was accompanied by the enhanced osteoclastogenic potential and oxidative stress in the aging process. **A**–**D** The plasma concentration of MT, oxidative stress markers including AOPPs, MDA and SOD-1 in young(3-month-old) mice and old (18-month-old) mice. Data represent mean ± S.D. of at least three independent experiments (n = 3 per group). **E**–**G** Western blot analysis of the TRAP and CTSK expression in the femoral metaphysis. **H**–**I** Representative images of TRAP staining for assessment of the number of TRAP-positive cells in the femoral metaphysis. Scale bar = 200 μm. **J**–**K** Flow cytometry analyses of the number and proportion of monocytes in the bone marrow cavity. Data represent mean ± S.D. of at least three independent experiments (n = 6 per group). **L** DCFH fluorescence analyses of intracellular ROS level in bone marrow monocytes (BMMs) from young and old mice. Data represent mean ± S.D. of at least three independent experiments (n = 3 per group). (M) Representative TRAP staining images of osteoclast differentiation of BMMs from young and old mice. Scale bar = 100 μm. **N** Quantification of TRAP + multinucleated cells (> 3 nuclei/cell) per field. **O** Representative rhodamine's Phalloidin staining for F-actin ring formation in BMMs from young and old mice. Scale bar = 50 μm. *p < 0.05, **p < 0.01, ***p < 0.001, ****p < 0.0001

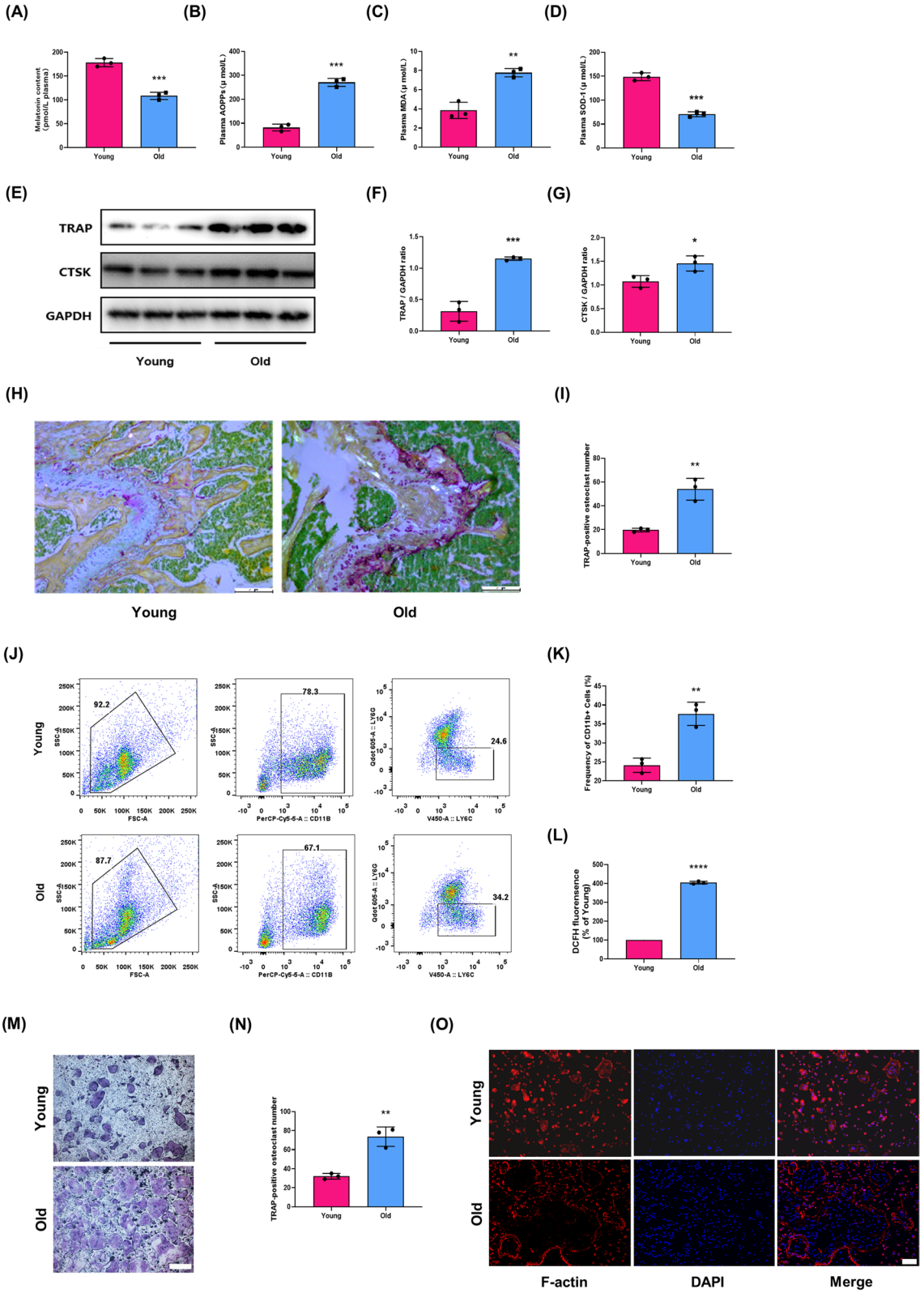

Fig. 1 (See legend on previous page.)

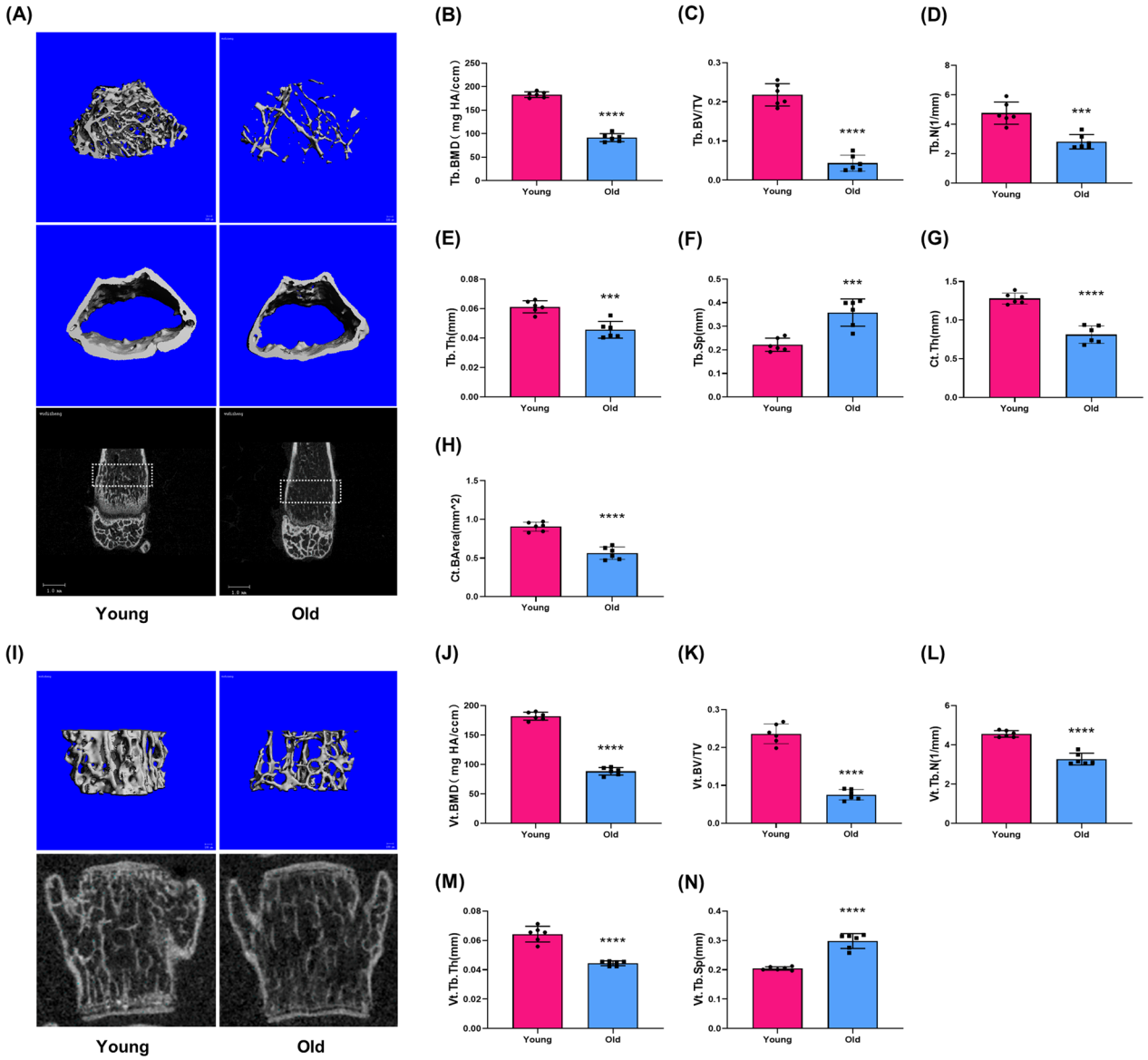

Fig. 2 Aged mice exhibited bone loss and deterioration of bone microstructure. **A** Representative micro-CT images of the distal femur from young (3-month-old) mice and old (18-month-old) mice. **B**–**H** Quantitative parameters in the distal femur, including bone mineral density (BMD), bone volume fraction (BV/TV), trabecular thickness (Tb/Vt.Th), trabecular number (Tb/Vt.N), trabecular separation (Tb/Vt.Sp), cortical bone thickness (Ct.th) and average cortical bone area (Ct.BArea). (I) Representative μCT images of L4 vertebral bodies. **J**–**N** Quantitative parameters in L4 vertebral bodies. Data represent mean ± S.D. of at least three independent experiments (n = 6 per group). ***p < 0.001; ****p < 0.0001

(See figure on next page.)

Fig. 3 MT suppressed osteoclastogenesis of BMMs from aged mice. **A** Representative TRAP staining images of osteoclast differentiation of BMMs from young mice, old mice and old mice with MT treatment. Scale bar = 100 μm. **B** Quantification of TRAP + multinucleated cells (> 3 nuclei/cell) per field. **C** Representative rhodamine's Phalloidin staining for F-actin ring formation in BMMs from three groups. Scale bar = 50 μm. **D** qRT-PCR analyses of the gene expression of TRAP and CTSK. (E–G) Western blot analysis of protein levels of TRAP and CTSK. (H) Representative electron microscop scanning for the formation of bone resorption pits. **I**–**K** Western blot analysis of protein levels of osteoclast-related transcription factors, c-Fos and NFATc1. *p < 0.05, **p < 0.01, ***p < 0.001, ****p < 0.0001 compared with the young group; $^{\#\#}$p < 0.01, $^{\#\#\#}$p < 0.001, $^{\#\#\#\#}$p < 0.0001 compared with the old group

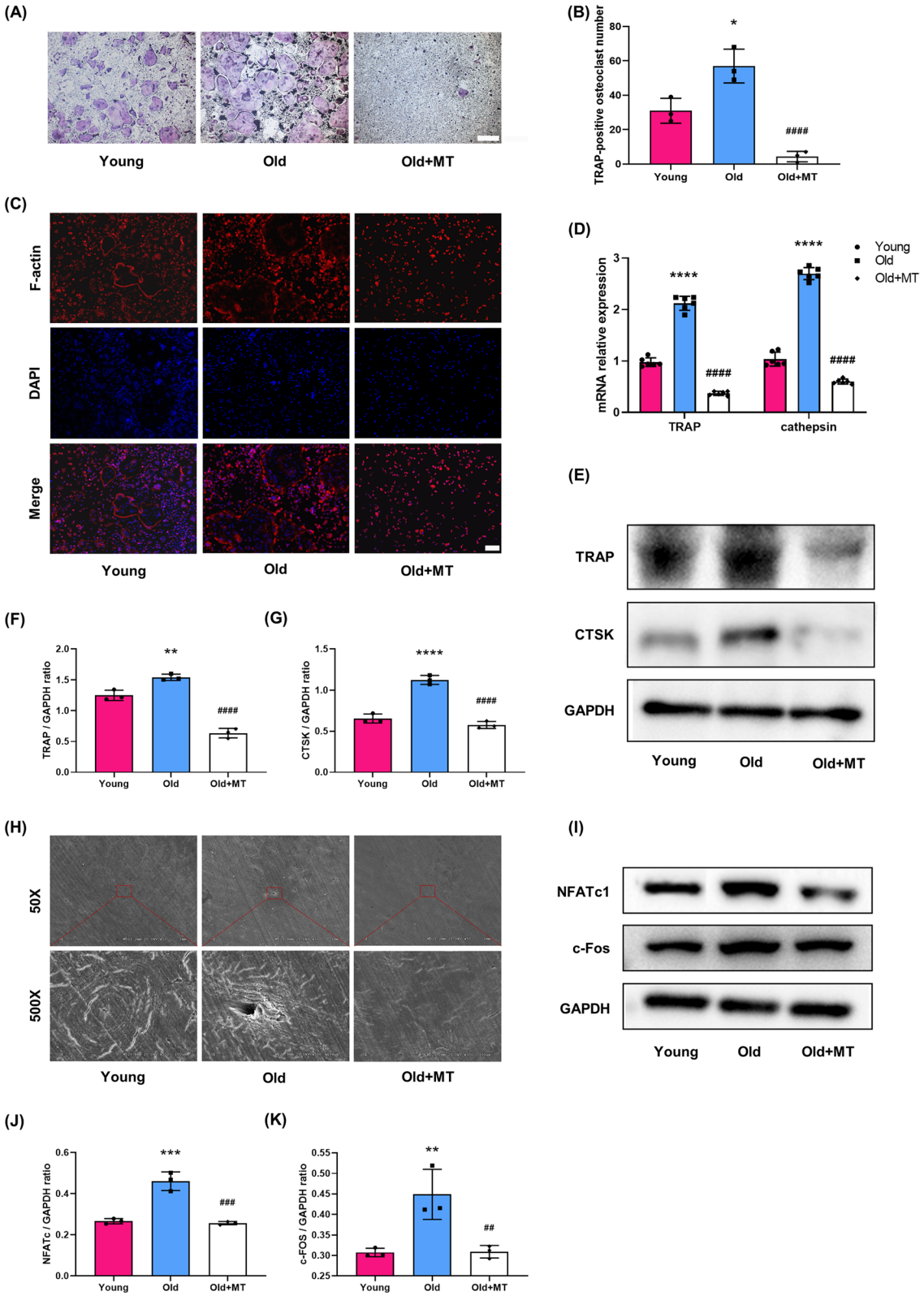

Fig. 3 (See legend on previous page.)

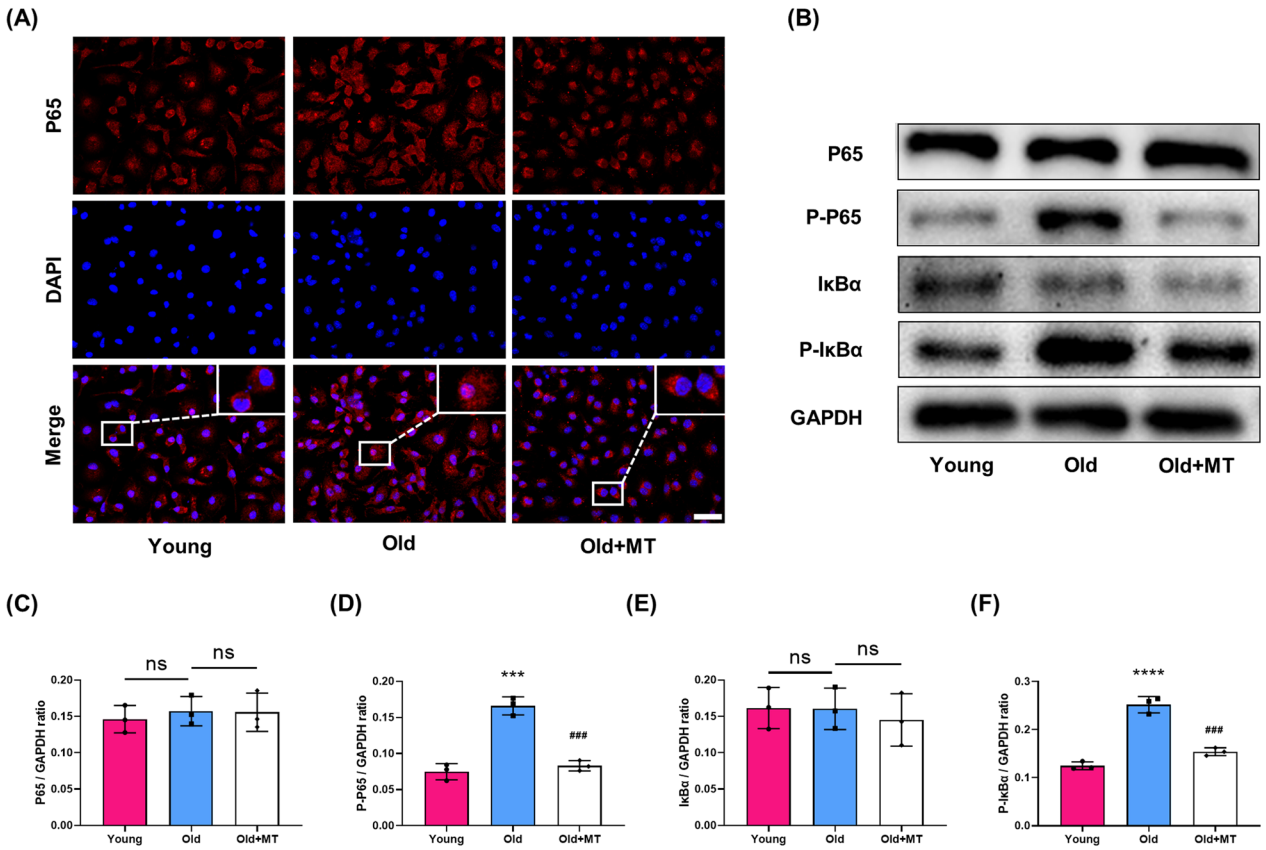

Fig. 4 MT inhibited phosphorylation of IκB and p65 in BMMs from aged mice. **A** Representative fluorescence images of p65 translocation from the cytoplasm to the nucleus. **B**–**F** Western blot analysis of protein levels of p65, P-p65, IκBα, P-IκBα. ***p < 0.001, ****p < 0.0001 compared with the young group; ###p < 0.001 compared with the old group; ns, not significant

L) in metaphysis of femur were also decreased in the MT treated group. We then evaluated the effect of MT on bone microstructure and bone mass. The μCT evaluation showed that MT treatment alleviated bone loss, deterioration of bone microstructure and the thinning of cortical bone in aged mice (Fig. 7). These results suggest that MT treatment attenuated oxidative stress, and suppressed osteoclastogenesis and bone loss in aged mice.

Discussion

Age-related bone loss increases susceptibility to osteoporosis and fragility fractures, compromising the quality of life in the elderly (Wan et al. 2021; Saul et al. 2022). Although anti-resorptive and anabolic drugs have been developed to address this condition, there are growing concerns about side effects and patient acceptance (Wei et al. 2020). Hence, alternative strategies may be necessary to prevent and treat age-related bone loss. MT is a neurohormone secreted by the pineal gland and known not only as regulator of the body's circadian rhythm but also as endogenous antioxidant (Galano et al. 2018; Rodriguez et al. 2004; Veneroso et al. 2009; Peyrot et al. 2008; Deng et al. 2006). Exogenous MT may alleviate the pathological process of osteoporosis by reducing oxidative stress and ROS production. Melatonin could antagonize adverse skeletal effects of oxidative stress through scavenging reactive nitrogen species (Oktem et al. 2006). Additionally, melatonin restores the osteogenic potential of bone marrow mesenchymal stem cells lost under conditions like osteoporosis through inhibition of H2O2-induced senescence (Chen et al. 2022). Furthermore, Melatonin improves trabecular microstructure in retinoic acid-induced osteoporosis mice by reducing oxidative stress through ERK/SMAD and NF-κB pathways (Wang et al. 2019). Besides the reported potential antioxidant effects of melatonin, research suggests that the serum MT level declines considerably with aging and contributes to the development of many age-related diseases (Claustrat et al. 2005), which underscores the importance of our findings. In this study, we demonstrated that MT level is linked with the changes in osteoclastogenesis and bone mass in the aging process, and MT supplementation can inhibit osteoclastogenesis and improve bone loss by enhanced antioxidant capacity.

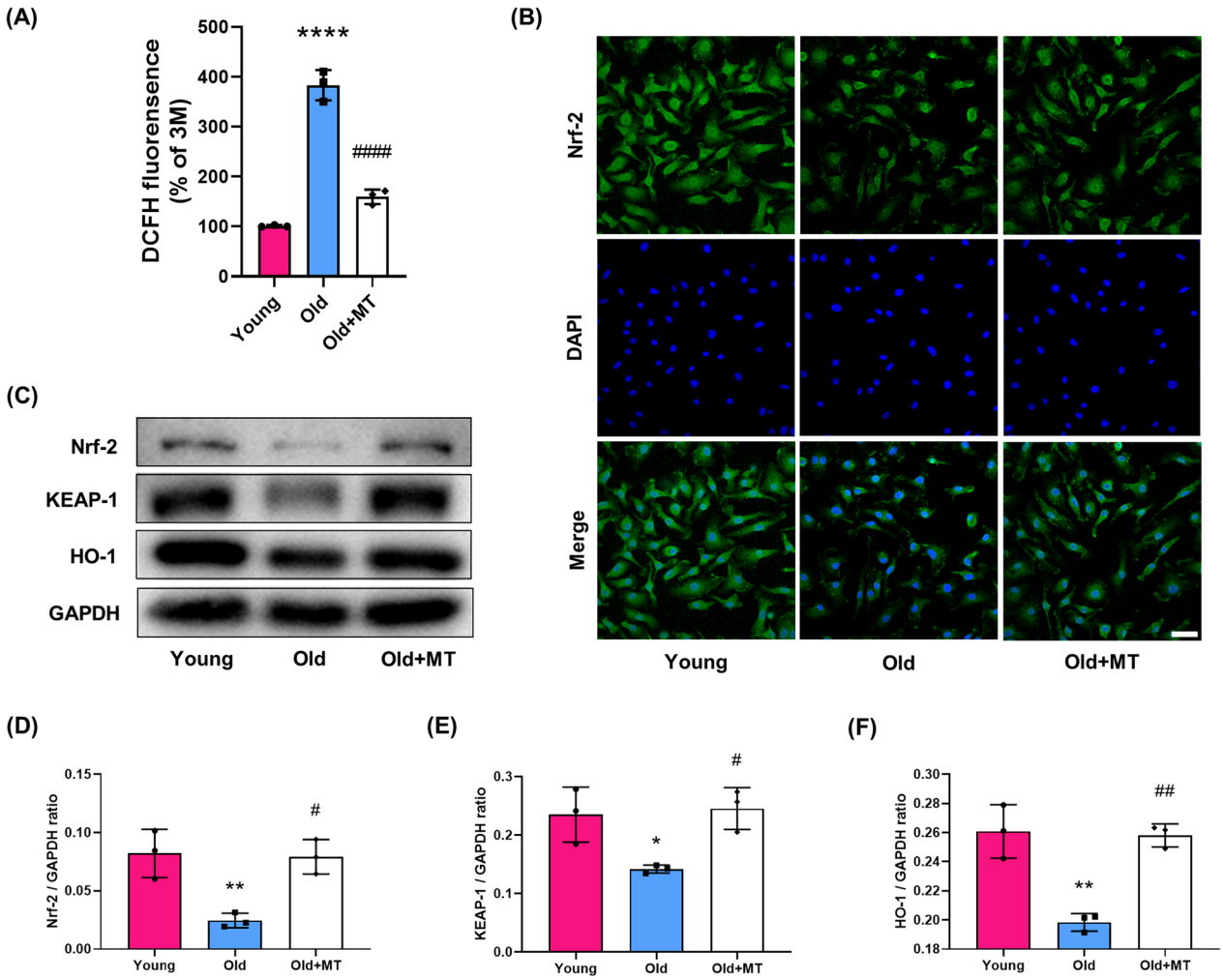

Fig. 5 MT enhanced the antioxidant capacity of BMMs from aged mice. **A** DCFH fluorensence analyses of intracellular ROS level in BMMs from young mice, old mice and old mice with MT treatment. Data represent mean ± S.D. of at least three independent experiments (n = 3 per group). **B** Representative fluorescence images of Nrf2 expression. **C**–**F** Western blot analysis of protein levels of Nrf2, Keap1 and HO-1. *p < 0.05, **p < 0.01, ****p < 0.0001 compared with the young group; $^{\#}$p < 0.05, $^{\#\#}$p < 0.01, $^{\#\#\#\#}$p < 0.0001 compared with the old group

Therefore, MT as an antioxidant may be a promising candidate for preventing or alleviating age-related bone loss.

Enhanced osteoclastogenesis is one of the major causes of age-related bone loss (Cao et al. 2005). The number of osteoclast progenitors increases with aging (Perkins et al. 1994), and these osteoclast progenitors show an increased ability to differentiate into mature osteoclasts and bone resorption (D'Amelio et al. 2005; Ziegler-Heitbrock. 2014). In this study, we found that aged mice showed an increased number of BMMs in the bone marrow cavity, higher capacity of osteoclastogenesis and lower bone mass compared with young mice. It was reported that MT can significantly inhibit osteoclast differentiation via attenuating intracellular ROS level in a dose-dependent manner at pharmacological concentrations (1–100 μM), but not at physiological concentrations (0.01–10 nM) (Zhou et al. 2017). Moreover, intraperitoneal injection of MT can prevent bone loss in mice with type 1 diabetes mellitus (Gong et al. 2022). This current study presented evidence that age-related decline of MT is associated with enhanced osteoclastogenesis and bone loss, and the MT challenge markedly suppresses osteoclastogenesis in vitro. Furthermore, MT supplementation exhibited a decrease of BMMs in the bone marrow cavity, and alleviated bone loss and deterioration of bone microstructure in aged mice. Therefore, MT plays an important role in bone homeostasis via the suppression of osteoclastogenesis and bone resorption activity.

Disruption of redox homeostasis may lead to oxidative stress and is involved in the aging process (Liguori

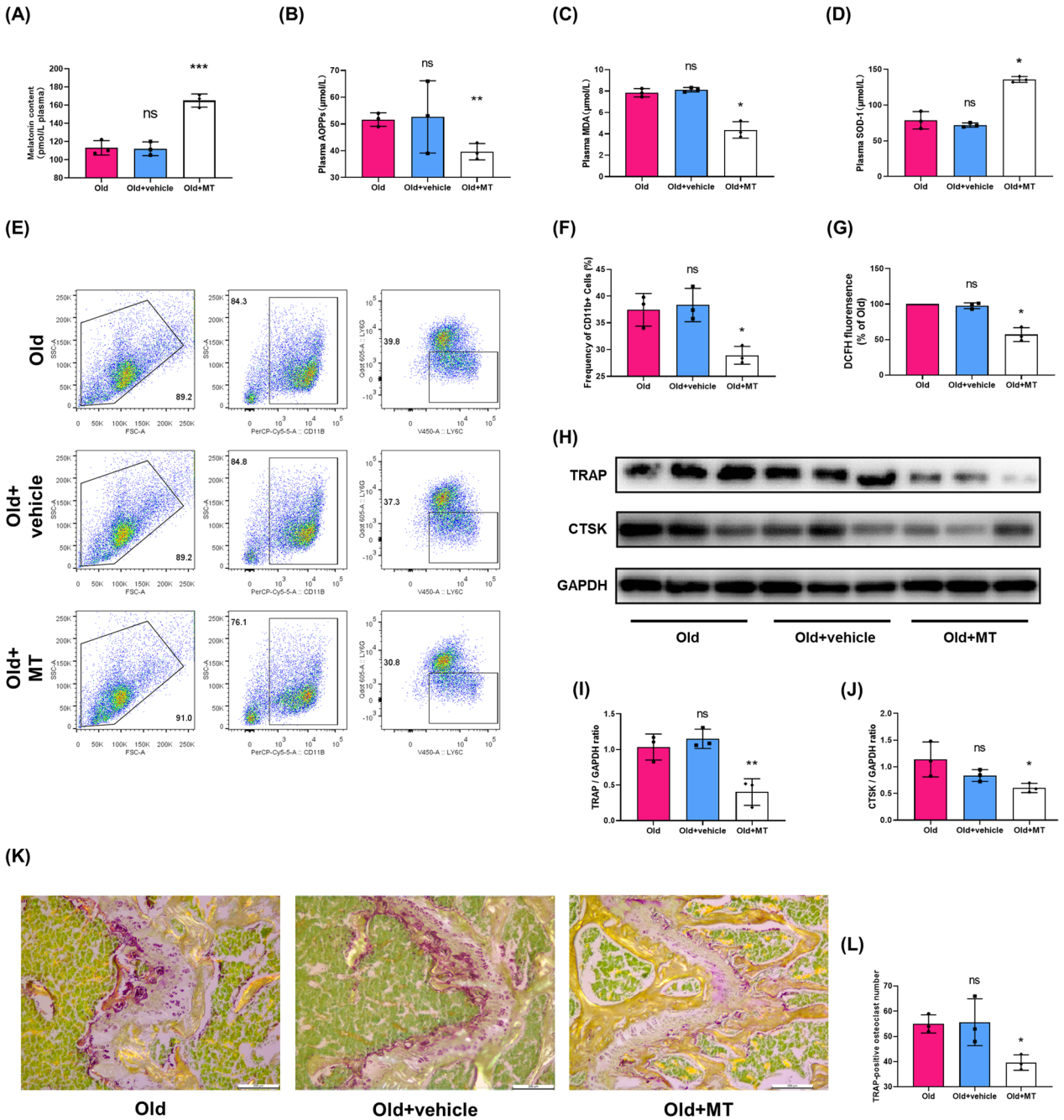

Fig. 6 MT supplementation attenuated oxidative stress and osteoclastagenesis in aged mice. **A**–**D** The plasma concentration of MT, AOPPs, MDA and SOD-1 in old mice, old mice with vehicle and old mice with MT treatment. **E**, **F** Flow cytometry analyses of the number and proportion of monocytes in the bone marrow cavity in three groups. **G** DCFH fluorescence analyses of intracellular ROS level in bone marrow monocytes (BMMs) from three groups. Data represent mean ± S.D. of at least three independent experiments (n = 3 per/group). **H**–**J** Western blot analysis of protein levels of TRAP and CTSK in the femoral metaphysis. **K**, **L** Representative images of TRAP staining for assessment of the number of TRAP-positive cells in the femoral metaphysis of old mice, old mice with vehicle and old mice with MT treatment. Scale bar = 200 μm. *p < 0.05, **p < 0.01, ***p < 0.001; ns, not significant

et al. 2018; Balaban et al. 2005). With aging, excessive oxidative stress has extensive negative effects on bone remodeling, thereby inducing bone loss as well as deterioration of bone quality and mechanical strength (Domazetovic et al. 2017). ROS act as intracellular signaling molecules involved in osteoclastogenesis.

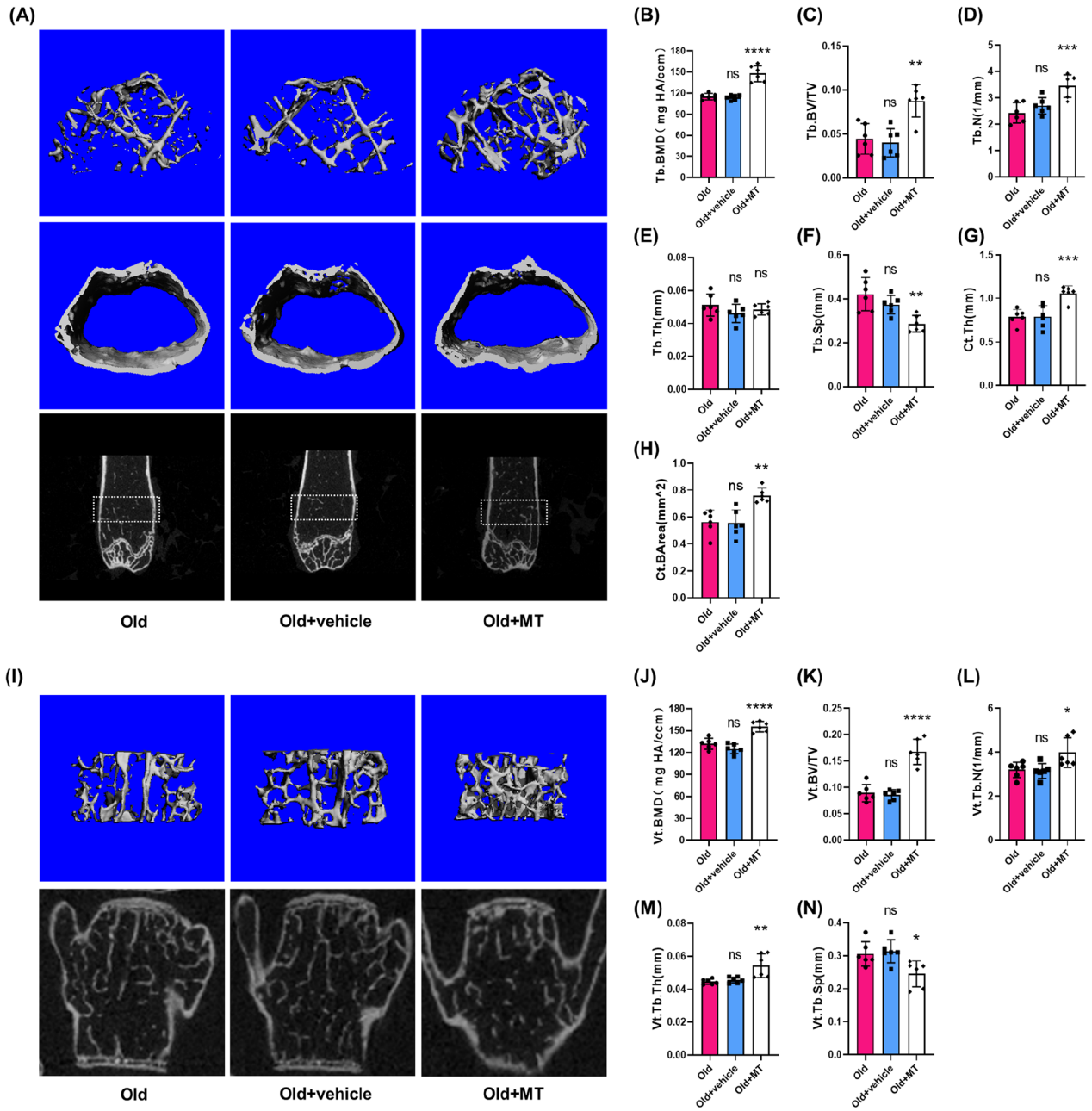

Fig. 7 MT supplementation alleviated the deterioration of bone microstructure and bone loss in aged mice. **A** Representative micro-CT images of the distal femur from old mice, old mice with vehicle and old mice with MT treatment. **B**–**H** Quantitative parameters in the distal femur, including bone mineral density (BMD), bone volume fraction (BV/TV), trabecular thickness (Tb/Vt.Th), trabecular number (Tb/Vt.N), trabecular separation (Tb/Vt.Sp), cortical bone thickness (Ct.th) and average cortical bone area (Ct.BArea). **I** Representative μCT images of L4 vertebral bodies. **J**–**N** Quantitative parameters in L4 vertebral bodies. Data represent mean ± S.D. of at least three independent experiments (n = 6 per group). *p < 0.05, **p < 0.01, ***p < 0.001, ****p < 0.0001; ns, not significant

Doxorubicin-induced bone loss is through a massive accumulation of ROS and nitrogen species leading to oxidative stress (Poudel et al. 2022). Moreover, Metastasis-associated protein 1 deficiency inhibited Nrf2 nuclear translocation and Increased intracellular ROS levels, leading to enhanced osteoclast formation (Feng et al. 2023). Accumulation of ROS is involved in enhanced osteoclastogenesis and bone resorption, leading to an imbalance in skeletal turnover and bone loss (Baek et al. 2010). In this study, elevated oxidative

stress, reflected in increased plasma AOPPs and MDA levels, was observed in aged mice. Moreover, the intracellular ROS level was significantly higher in BMMs from aged mice than that in young mice. MT supplementation can markedly reverse osteoclastogenesis and bone loss by alleviating oxidative stress. Therefore, MT influences osteoclastogenesis via regulating redox homeostasis.

The present study had several limitations. First, age-related bone loss, a highly complex process, was investigated only in young and old mice. This model may not fully reflect its complexities in humans. Second, we focus on the impact of MT on osteoclastogenesis but not on osteogenesis. Actually, bone loss results from an imbalance between osteoblastic bone formation and osteoclastic bone resorption in the natural aging process (Sfeir et al. 2022). Previous study has demonstrated that MT can enhance osteogenic differentiation of bone marrow mesenchymal stem cells and restore oxidative stress-inhibited osteogenesis (Lee et al. 2018). In our study, MT treatment may improve bone mass in old mice in part by restoring osteogenesis and bone formation. Furthermore, circadian rhythm disruption easily leads to bone loss and osteoporosis (Swanson et al. 2017). Evidence has shown that the circadian system may be a promising intervention for the treatment of abnormal bone metabolism (Song et al. 2018). It is necessary to further clarify the effect of MT on age-related bone loss by regulating the body's circadian rhythm.

Conclusions

Our results suggest that MT level declines with aging, which is associated with disruption of redox homeostasis. Age-related decline of MT contributes to enhanced osteoclastogenesis and bone loss. Exogenous MT supplementation can attenuate osteoclastogenesis and improve bone loss through enhancing antioxidant capacity. Collectively, MT as a dietary supplementation and/or medicinal drug is beneficial in the prevention and treatment of age-related bone loss and senile osteoporosis.

Supplementary Information

The online version contains supplementary material available at https://doi.org/10.1186/s10020-024-00779-x.

Additional file 1: Figure S1. The effects of different concentrations of MT on the osteoclastogenesis of BMMs. (A) Representative TRAP staining images of osteoclast differentiation of BMMs in vitro after treatment of MT at different concentrations. (B) Representative rhodamine's Phalloidin staining for F-actin ring formation in BMMs. (C) Cell proliferation was quantified at separate time points of 1, 2, 3, 4, 5 and 6 d and showed no significant differences between MT treated and untreated groups of BMMs. (D) DCFH fluorescence analyses of intracellular ROS level in BMMs after treatment of MT at different concentrations. Data represent mean ± S.D. of at least three independent experiments (n = 3 per/group). *p < 0.05, **p < 0.01.

Acknowledgements
Not applicable.

Author contributions
Z-MZ and D-ZW conceived and designed the project. D-ZW performed the majority of the study and analyzed data. D-ZW and G-ZZ worked on the preparation of the manuscript. KZ, J-WG, G-XC, H-ZL, CT, Y-SH and J-SZ provided critical feedback and helped to this research work. All authors approved the final manuscript.

Funding
This study was funded in part by the GuangDong Basic and Applied Basic Research Foundation (2019A1515012075).

Availability of data and materials
The data and materials of the study can be obtained from the corresponding author upon request.

Declarations

Ethics approval and consent to participate
All animal experiments were approved by the Laboratory Animal Care and Use Committee of Nanfang Hospital, Southern Medical University (NFYY-2021-0420), and the use of animals in our experiments was consistent with ethical requirements.

Consent for publication
Not applicable.

Competing interests
The authors declare no competing interests.

Author details
[1]Division of Spine Surgery, Department of Orthopaedics, Nanfang Hospital, Southern Medical University, 1838 North Guangzhou Avenue, Guangzhou 510515, China. [2]Department of Orthopaedics, First Affiliated Hospital of Gannan Medical University, Ganzhou 341000, China.

Received: 18 September 2023 Accepted: 4 January 2024
Published online: 12 January 2024

References

Baek KH, Oh KW, Lee WY, et al. Association of oxidative stress with postmenopausal osteoporosis and the effects of hydrogen peroxide on osteoclast formation in human bone marrow cell cultures. Calcif Tissue Int. 2010;87(3):226–35.
Balaban RS, Nemoto S, Finkel T. Mitochondria, oxidants, and aging. Cell. 2005;120(4):483–95.
Cao JJ, Wronski TJ, Iwaniec U, Phleger L, Kurimoto P, Boudignon B, et al. Aging increases stromal/osteoblastic cell-induced osteoclastogenesis and alters the osteoclast precursor pool in the mouse. J Bone Miner Res. 2005;20(9):1659–68.
Chen W, Chen X, Chen AC, et al. Melatonin restores the osteoporosis-impaired osteogenic potential of bone marrow mesenchymal stem cells by preserving SIRT1-mediated intracellular antioxidant properties. Free Radic Biol Med. 2020;146:92–106.
Chen W, Lv N, Liu H, Gu C, Zhou X, Qin W, et al. Melatonin improves the resistance of oxidative stress-induced cellular senescence in osteoporotic bone marrow mesenchymal stem cells. Oxid Med Cell Longev. 2022;2022:1–2.
Claustrat B, Brun J, Chazot G. The basic physiology and pathophysiology of melatonin. Sleep Med Rev. 2005;9(1):11–24.

Compston JE, Mcclung MR, Leslie WD. Osteoporosis. Lancet. 2019;393(10169):364–76.
Cui J, Shibata Y, Zhu T, Zhou J, Zhang J. Osteocytes in bone aging: advances, challenges, and future perspectives. Ageing Res Rev. 2022;77: 101608.
D'Amelio P, Grimaldi A, Pescarmona GP, Tamone C, Roato I, Isaia G. Spontaneous osteoclast formation from peripheral blood mononuclear cells in postmenopausal osteoporosis. FASEB J. 2005;19(3):410–2.
Deng WG, Tang ST, Tseng HP, Wu KK. Melatonin suppresses macrophage cyclooxygenase-2 and inducible nitric oxide synthase expression by inhibiting p52 acetylation and binding. Blood. 2006;108(2):518–24.
Domazetovic V, Marcucci G, Iantomasi T, et al. Oxidative stress in bone remodeling role of antioxidants. Clin Cases Miner Bone Metab. 2017;14(2):209–16.
Feng M, Liu L, Qu Z, Zhang B, Wang Y, Yan L, et al. CRISPR/Cas9 knockout of MTA1 enhanced RANKL-induced osteoclastogenesis in RAW264.7 cells partly via increasing ROS activities. J Cell Mol Med. 2023;27(5):701.
Fishbein AB, Knutson KL, Zee PC. Circadian disruption and human health. J Clin Invest. 2021; 131(19).
Galano A, Tan DX, Reiter RJ. Melatonin: a versatile protector against oxidative DNA damage. Molecules. 2018;23(3):530.
Gong Z, Da W, Tian Y, Zhao R, Qiu S, Wu Q, et al. Exogenous melatonin prevents type 1 diabetes mellitus-induced bone loss, probably by inhibiting senescence. Osteoporos Int. 2022;33(2):453–66.
Hyeon S, Lee H, Yang Y, Jeong W. Nrf2 deficiency induces oxidative stress and promotes RANKL-induced osteoclast differentiation. Free Radic Biol Med. 2013;65:789–99.
Jevon M, Sabokbar A, Fujikawa Y, Hirayama T, Neale SD, Wass J, et al. Gender- and age-related differences in osteoclast formation from circulating precursors. J Endocrinol. 2002;172(3):673–81.
Kanzaki H, Shinohara F, Itohiya K, Yamaguchi Y, Katsumata Y, Matsuzawa M, et al. RANKL induces Bach1 nuclear import and attenuates Nrf2-mediated antioxidant enzymes, thereby augmenting intracellular reactive oxygen species signaling and osteoclastogenesis in mice. FASEB J. 2017;31(2):781–92.
Kedziora-Kornatowska K, Szewczyk-Golec K, Czuczejko J, et al. Antioxidative effects of melatonin administration in elderly primary essential hypertension patients. J Pineal Res. 2008;45(3):312–7.
Khan S, Adhikari JS, Rizvi MA, Chaudhury NK. Melatonin attenuates Co γ-ray-induced hematopoietic, immunological and gastrointestinal injuries in C57BL/6 male mice. Environ Toxicol. 2017;32(2):501.
Kim JH, Kim N. Regulation of NFATc1 in osteoclast differentiation. J Bone Metab. 2014;21(4):233–41.
Lee NK, Choi YG, Baik JY, Han SY, Jeong DW, Bae YS, et al. A crucial role for reactive oxygen species in RANKL-induced osteoclast differentiation. Blood. 2005;106(3):852–9.
Lee S, Le NH, Kang D. Melatonin alleviates oxidative stress-inhibited osteogenesis of human bone marrow-derived mesenchymal stem cells through AMPK activation. Int J Med Sci. 2018;15(10):1083–91.
Li T, Jiang S, Lu C, Yang W, Yang Z, Hu W, et al. Melatonin: another avenue for treating osteoporosis? J Pineal Res. 2019;66(2): e12548.
Li X, Li B, Shi Y, Wang C, Ye L. Targeting reactive oxygen species in stem cells for bone therapy. Drug Discov Today. 2021;26(5):1226–44.
Liguori I, Russo G, Curcio F, Bulli G, Aran L, Della-Morte D, et al. Oxidative stress, aging, and diseases. Clin Interv Aging. 2018;13:757–72.
Liu Y, Wang C, Wang G, Sun Y, Deng Z, Chen L, et al. Loureirin B suppresses RANKL-induced osteoclastogenesis and ovariectomized osteoporosis via attenuating NFATc1 and ROS activities. Theranostics. 2019;9(16):4648–62.
Ma H, Wang X, Zhang W, Li H, Zhao W, Sun J, et al. Melatonin suppresses ferroptosis induced by high glucose via activation of the Nrf2/HO-1 signaling pathway in type 2 diabetic osteoporosis. Oxid Med Cell Longev. 2020;2022:1–18.
Manolagas SC. From estrogen-centric to aging and oxidative stress: a revised perspective of the pathogenesis of osteoporosis. Endocr Rev. 2010;31(3):266–300.
Moller A, Delaisse JM, Olesen JB, Madsen JS, Canto LM, Bechmann T, et al. Aging and menopause reprogram osteoclast precursors for aggressive bone resorption. Bone Res. 2020;8:27.
Munmun F, Witt-Enderby PA. Melatonin effects on bone: Implications for use as a therapy for managing bone loss. J Pineal Res. 2021;71(1): e12749.
Ni S, Qian Z, Yuan Y, Li D, Zhong Z, Ghorbani F, et al. Schisandrin A restrains osteoclastogenesis by inhibiting reactive oxygen species and activating Nrf2 signalling. Cell Prolif. 2020;53(10): e12882.
Oktem G, Uslu S, Vatansever SH, Aktug H, Yurtseven ME, Uysal A. Evaluation of the relationship between inducible nitric oxide synthase (iNOS) activity and effects of melatonin in experimental osteoporosis in the rat. Surg Radiol Anat. 2006;28(2):157–62.
Perkins SL, Gibbons R, Kling S, Kahn AJ. Age-related bone loss in mice is associated with an increased osteoclast progenitor pool. Bone. 1994;15(1):65–72.
Peyrot F, Ducrocq C. Potential role of tryptophan derivatives in stress responses characterized by the generation of reactive oxygen and nitrogen species. J Pineal Res. 2008;45(3):235–46.
Poudel S, Martins G, Cancela ML, Gavaia PJ. Regular supplementation with antioxidants rescues doxorubicin-induced bone deformities and mineralization delay in Zebrafish. Nutrients. 2022;14(23):4959.
Rasmussen DD, Mitton DR, Larsen SA, Yellon SM. Aging-dependent changes in the effect of daily melatonin supplementation on rat metabolic and behavioral responses. J Pineal Res. 2001;31(1):89–94.
Rodriguez C, Mayo JC, Sainz RM, Antolin I, Herrera F, Martin V, et al. Regulation of antioxidant enzymes: a significant role for melatonin. J Pineal Res. 2004;36(1):1–9.
Satomura K, Tobiume S, Tokuyama R, Yamasaki Y, Kudoh K, Maeda E, et al. Melatonin at pharmacological doses enhances human osteoblastic differentiation in vitro and promotes mouse cortical bone formation in vivo. J Pineal Res. 2007;42(3):231–9.
Saul D, Khosla S. Fracture healing in the setting of endocrine diseases, aging, and cellular senescence. Endocr Rev. 2022;43:984.
Sfeir JG, Drake MT, Khosla S, Farr JN. Skeletal aging. Mayo Clin Proc. 2022;97(6):1194–208.
Shao J, Liu S, Zhang M, Chen S, Gan S, Chen C, et al. A dual role of HIF1alpha in regulating osteogenesis-angiogenesis coupling. Stem Cell Res Ther. 2022;13(1):59.
Song C, Wang J, Kim B, Lu C, Zhang Z, Liu H, et al. Insights into the role of circadian rhythms in bone metabolism: a promising intervention target? Biomed Res Int. 2018;2018:9156478.
Swanson CM, Shea SA, Wolfe P, Cain SW, Munch M, Vujovic N, et al. Bone turnover markers after sleep restriction and circadian disruption: a mechanism for sleep-related bone loss n humans. J Clin Endocrinol Metab. 2017;102(10):3722–30.
Veneroso C, Tunon MJ, Gonzalez-Gallego J, Collado PS. Melatonin reduces cardiac inflammatory injury induced by acute exercise. J Pineal Res. 2009;47(2):184–91.
Wan M, Gray-Gaillard EF, Elisseeff JH. Cellular senescence in musculoskeletal homeostasis, diseases, and regeneration. Bone Res. 2021;9(1):41.
Wang X, Liang T, Zhu Y, Qiu J, Qiu X, Lian C, et al. Melatonin prevents bone destruction in mice with retinoic acid–induced osteoporosis. Mol Med. 2019;25(1).
Wei H, Xu Y, Wang Y, Xu L, Mo C, Li L, et al. Identification of fibroblast activation protein as an osteogenic suppressor and anti-osteoporosis drug target. Cell Rep. 2020;33(2): 108252.
Zhou L, Chen X, Yan J, Li M, Liu T, Zhu C, et al. Melatonin at pharmacological concentrations suppresses osteoclastogenesis via the attenuation of intracellular ROS. Osteoporos Int. 2017;28(12):3325–37.
Zhu SY, Zhuang JS, Wu Q, Liu ZY, Liao CR, Luo SG, et al. Advanced oxidation protein products induce pre-osteoblast apoptosis through a nicotinamide adenine dinucleotide phosphate oxidase-dependent, mitogen-activated protein kinases-mediated intrinsic apoptosis pathway. Aging Cell. 2018;17(4): e12764.
Zhuang J, Chen X, Cai G, Wu D, Tu C, Zhu S, et al. Age-related accumulation of advanced oxidation protein products promotes osteoclastogenesis through disruption of redox homeostasis. Cell Death Dis. 2021;12(12):1160.
Ziegler-Heitbrock L. Monocyte subsets in man and other species. Cell Immunol. 2014;289(1–2):135–9.

Publisher's Note